

# A mutation in *CsKTN1* for the Katanin p60 protein results in miniature plant in cucumber, *Cucumis sativus* L.

MengFei Song, WenYuan Fu, YuHui Wang, Feng Cheng, MengRu Zhang, JinFeng Chen\*, and QunFeng Lou\*

State Key Laboratory of Crop Genetics and Germplasm Enhancement, College of Horticulture, Nanjing Agricultural University, Nanjing 210095, China

\* Corresponding authors, E-mail: [jfchen@njau.edu.cn](mailto:jfchen@njau.edu.cn); [qflou@njau.edu.cn](mailto:qflou@njau.edu.cn)

## Abstract

Katanin, a microtubule shearing protein, plays an important role in plant architecture formation. However, little is known about its mechanisms in regulating plant architecture in cucumber. In the present study, through EMS mutagenesis, we identified a novel *micro-plant* (*mp*) mutant in the North China type inbred line CCMC that may be of value for cucumber breeding. The size and number of stem cells were altered in the *mp* mutant. Through bulked segregant analysis (BSA) sequencing approach combined with genetic mapping, the *mp* locus was delimited to an interval of 130.9-kb. Multiple lines of evidence suggested that the *mp* mutation is due to a single nucleotide polymorphism in *Csa7G435510* that is predicted to encode the Katanin p60 subunit protein (*CsKTN1*). The expression levels of *CsKTN1* decreased significantly in all tissues except the tendril of *mp* mutant. Subcellular localization showed that both wild-type and mutant *CsKTN1* proteins were located in cell membrane, cytoplasm and nucleus of tobacco leaf cells. The mutant protein lost part of its ability to bind and shear microtubule *in vitro*. These findings provide new insight into the regulatory function of microtubule-shearing protein, Katanin p60, in plant architecture of cucumber.

**Citation:** Song M, Fu W, Wang Y, Cheng F, Zhang M, et al. 2022. A mutation in *CsKTN1* for the Katanin p60 protein results in miniature plant in cucumber, *Cucumis sativus* L.. *Vegetable Research* 2:3 <https://doi.org/10.48130/VR-2022-0003>

## INTRODUCTION

Plant architecture refers to the morphological characteristics and spatial distribution of plants. Distinct plant architecture may change the distribution of solar radiation in the population, affecting carbon assimilation and dry matter accumulation of photosynthetic organs, ultimately resulting in different yields. It also directly determines the amount of labor input in cultivation management. Plants with ideal architecture can have beneficial characteristics including reduced area required for cultivation, reduced labor needs, enhanced light utilization, and increased yield. Crops such as rice<sup>[1]</sup>, wheat<sup>[2]</sup> and maize<sup>[3]</sup> have all benefited from genetic modification of plant architecture. The green revolution was primarily due to the finding and use of semi-dwarf genes in rice and wheat. Many of the genes underlying plant architecture related traits have been cloned<sup>[4,5]</sup>.

As a climbing crop, cucumber (*Cucumis sativus* L.) has the indeterminate growth habit under optimum greenhouse management. Reducing plant height (vine length) and organ size can increase plant density and productivity. To address this trait, eight associated loci/genes have been reported and cloned, including *CsCLAVATA1* (*dwarf*, *dw*), *CsVFB1* (*short internode*, *si*), *CsCullin1* (*compact*, *cp*), *CsCKX* (*compact-1*, *cp-1*), *CsCYP85A1* (*super compact-1*, *scp-1*) and *CsDET2* (*super compact-2*, *scp-2*)<sup>[6]</sup>. These mutants exhibited reduced internode length or compact growth habit and were reported to be mainly involved in CLAVATA signaling pathway and phytohormones biosynthesis pathway including brassinosteroid (BR), auxin, cytokinin, and jasmonic acid<sup>[7-11]</sup>. A tendril-less mutant (*td-1*) obtained from the EMS-induced mutagenesis population was found to have significantly reduced vine length although the

regulatory mechanism remains unknown<sup>[12]</sup>. Three loci related to leaf size were mapped for the study of small organs in cucumber: *little leaf* (*ll*), *little leaf 2* (*ll-2*) and *small and cordate leaf 1* (*scl-1*)<sup>[13,14]</sup>. Among them, *scl-1* showed significant reduction in leaf length and width, whereas *ll* and *ll-2* mutants showed shrunken phenotypes in more organs such as leaves, flowers, seeds, and fruits. Although a number of mutants have been reported, the currently available mutants or genotypes have not been applied to cucumber breeding with modified plant architecture, which is perhaps due to their extreme phenotypes or the vague understanding of their regulatory mechanisms

The size and shape of cells could be determined by the depolymerization state of microtubules, which would affect the plant architecture<sup>[15]</sup>. As one of the microtubule shearing proteins, Katanin protein is a heterodimer composed of two subunits, p60 and p80<sup>[16]</sup>. Katanin p60 subunit protein which belongs to the AAA protein family, could catalyze the hydrolysis of ATP and shear microtubules under the action of ROP6-RIC1 signaling pathway<sup>[17]</sup>. Its cleavage activity is mainly regulated by several factors including Katanin p80 subunit, intracellular ATP and Ca<sup>2+</sup> content, light signal induction, phytohormones, and microtubule morphology<sup>[18]</sup>. Katanin heterodimer was directed by Katanin p80 microtubule cleavage site for specific microtubule recognition to complete the cleavage<sup>[19]</sup>. In addition, the Katanin-mediated severing could be antagonized by augmin protein at microtubule crossovers<sup>[20]</sup>. In post-translational regulation, Katanin p60 was ubiquitinated by MAB1 (MATH-BTB1) through decoupling with E3 ubiquitin ligase complex containing CLU-3<sup>[21]</sup>.

Mutations in Katanin p60 coding genes may disrupt the morphogenesis during plant growth by affecting cell division

plane orientation<sup>[15,22]</sup>. A total of seven defective loci in Katanin p60 protein were reported including *BOT1*, *DGL1*, *ERH3*, *FRA2/AtKTN1*, *FRC2*, *KTN1*, and *LUE1/AtKSS*, which were identified in *Arabidopsis* (six mutations allelic of the same locus) and rice (one locus)<sup>[23–28]</sup>. These mutants had varying degrees of microtubule and cell growth defects such as reduced cell length or impaired cell elongation, abnormal cell wall location or reduced cellulose content, and cell division plane orientation defects<sup>[22]</sup>. As a result, both vegetative and reproductive organs showed irregular growth patterns, such as shorter internodes, compact organs, root radial swelling, abnormally shaped hypophysis, sterile flowers and malformed ovule development<sup>[22]</sup>. In conclusion, microtubule severing by Katanin p60 displayed a broad range of association with cellular and developmental processes in plants.

Previous studies indicated that there is a link between plant architecture and Katanin protein. In the present study, we identified a micro-plant cucumber mutant *mp* with small organ phenotype caused by defects in Katanin protein. This mutant is a novel material to study its function and application in plant architecture breeding in horticulture plants, especially for climbing plants such as cucurbit crops. To increase the potential value of cucumber plant architecture breeding, we investigated the molecular mechanism and biological function of microtubule-shearing protein Katanin p60 involved in cell morphogenesis and plant architecture.

## MATERIALS AND METHODS

### Plant materials

Micro-plant mutant (*mp*) displaying reduced organ size was obtained from the M<sub>2</sub> generation of ethyl methanesulfonate (EMS)-induced mutagenesis population. The donor line for mutagenesis was CCMC (Changchunmici), a North China fresh market type with normal plant architecture (Fig. 1). Another normal line 'Hazerd', a European greenhouse inbred line with wild type plant architecture, was used for developing a

segregation population with *mp* mutant. The following traits were measured to determine the accurate phenotype, hypocotyl length (one true-leaf stage), plant height, internode length (10 true-leaf stage), leaf length, leaf width, petiole length (10<sup>th</sup> true-leaf), ovary length (flowering stage), commercial fruit length (7 d after pollination) and mature fruit length (40 d after pollination).

Several F<sub>2</sub> populations were developed to investigate the inheritance of *mp* including F<sub>2</sub> populations obtained separately from the crosses between CCMC and *mp* mutant, 'Hazerd' and *mp* mutant. All cucumber germplasm resources used in this research were obtained from the Laboratory of Cucurbitae Genetic and Germplasm Enhancement in the College of Horticulture, Nanjing Agricultural University. The plant materials were grown and phenotyped in greenhouses at Baima Cucumber Research Station of Nanjing Agricultural University, Nanjing, China.

### Scanning electron microscopy

Scanning electron microscopy was performed according to the protocol as described previously<sup>[29]</sup> with minor modification. The main stems of the second internode of CCMC and *mp* mutant plants at 10 true-leaf stage were investigated under a scanning electronic microscope (SEM). Firstly, the tissue samples were flushed with 1.0% formaldehyde to remove the surface wax powder and cut longitudinally into 2 mm × 5 mm size, then quickly fixed in 4% glutaraldehyde phosphate buffer (pH = 6.8) for 24 h. The fixed samples were dehydrated in a graded ethanol series (30%, 50%, 70%, 80%, 90%, and 100%) and critical-point drying. A Hitachi JSM-6360LV scanning electron microscope was used for sample observation. The cell length, width and number were calculated by ImageJ software.

### Paraffin sectioning

Paraffin sectioning was performed according to the protocol as described previously<sup>[30]</sup> with minor modification. Ovaries of WT and *mp* mutant plants grown under the same conditions were sampled separately, and then fixed in 50% FAA fixation solution (50% ethanol, 10% formalin, 5% acetic acid) for at least

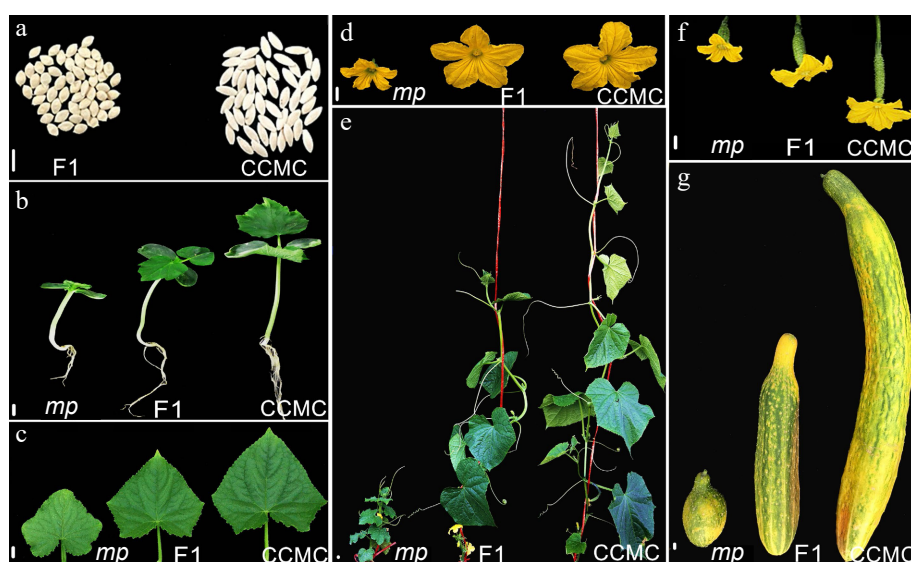


**Fig. 1** Morphological characterization of CCMC and *mp* mutant. Representative photographs of *mp* mutant cucumber plants showing miniaturized development in (a) seed, (b) hypocotyl and root, (c) the 1<sup>st</sup> true leaf, (d) male flower, (e) the whole plant expanded 10 true-leaf stage, (f) female flower and ovary, and (g) mature fruit. Scale bar = 10 mm.

The role of *CsKTN1* in cucumber

16 h and embedded in paraffin. Transverse sections of 3 mm thickness were mounted in neutral balsam. Neutral balsam was melted, and tissue was incubated three times in balsam bath. Melted balsam was poured into a block mold together with the tissue and allowed to cool. Longitudinal sections were cut with 8  $\mu\text{m}$  thickness and then fixed on micro slides and stained with 1% hematoxylin for 3–5 min. Finally, haematoxylin eosin (HE) staining results were examined and photographed using an OLYMPUS BX53 fluorescence microscope.

**Measurement of photosynthetic parameters**

Photosynthetic parameters including net photosynthetic rate (Pn), stomatal conductance (Gs), intercellular CO<sub>2</sub> concentration (Ci), transpiration rate (E) and chlorophyll fluorescence parameters Fv/Fm of CCMC and *mp* mutant plants were measured using the US-made LI-6800 portable photosynthesis measurement system. All plants were grown in a plant culture incubator at 28 °C day / 24 °C night temperature and 10,000 Lux light intensity. The first fully expanded true leaf was selected to measure photosynthetic parameters at 8–10 in the morning. Ten leaves for each material were selected as biological repeats.

**Genetic mapping of *mp* candidate gene**

Among 485 F<sub>2</sub> individuals obtained from the cross between CCMC and *mp* mutant, equal amounts of DNA from 21 and 24 individuals with mutant and normal plant types were bulked, respectively. The DNA was extracted by CTAB method. A modified BSA-seq method<sup>[31]</sup> was used to map the *mp* locus. The two bulks were subjected to whole genome resequencing using the Illumina HiSeq 2500 (500 bp) platform. CCMC was re-sequenced in our previous study<sup>[32]</sup>. Reads from both bulks were independently aligned to the CCMC consensus sequence reads for variants calling. SNP index,  $\Delta$  (SNP index), and the *p*-values were calculated to determine the candidate region. The average SNP index of SNPs in a genomic interval was calculated using sliding window analysis with 1 Mb window size and 10 kb increment.

Due to the low level of polymorphism between *mp* and CCMC, a linkage group for target chromosome was constructed using the 273 F<sub>2</sub> population from *mp* x Hazerd. To identify more recombinants in the target region, additional 708 F<sub>2</sub> individuals from the same cross were employed. Plant genotypes were determined by identification of molecular markers. 'Hazerd' was re-sequenced in our previous study<sup>[32]</sup>. Indel (Insertion/Deletion) and SNP markers were developed within the preliminary interval using re-sequenced data of 'Hazerd' and CCMC. The candidate SNPs in refined region were annotated using the Cucumber Genome Database (<http://cucurbitgenomics.org>)<sup>[33]</sup>. All primer sequences are listed in Supplemental Table S1.

**Sequence analysis, annotation, and identification of the *mp* candidate gene**

Total RNA was extracted from leaves of CCMC and *mp* mutant plants using Trizol method. cDNA synthesis was performed using a Prime Script™ RT Reagent Kit (TaKaRa). The coding sequences of the candidate gene from CCMC and *mp* mutant were cloned and sequenced by Sanger sequencing. Functional annotations of candidate genes were acquired from Cucumber Genome Database (<http://cucurbitgenomics.org>) and NCBI (National Center for Biotechnology Information) databases ([www.ncbi.nlm.nih.gov](http://www.ncbi.nlm.nih.gov)). The homologous amino acid sequences of predicted proteins from nine plant species were downloaded from NCBI database ([www.ncbi.nlm.nih.gov](http://www.ncbi.nlm.nih.gov)) (NCBI

GenBank No: *Cucumis melo*: XP\_016902686.1; *Gossypium hirsutum*: XP\_016739756.1; *Arabidopsis thaliana*: BAB87822.1; *Solanum lycopersicum*: XP\_004241721.1; *Nicotiana tabacum*: XP\_016456600.1; *Oryza sativa*: XP\_015622511.1; *Sorghum bicolor*: XP\_002456154.1; *Brachypodium distachyon*: XP\_003569573.1; *Hordeum vulgare*: KAE8818098.1). MEGA 7.0.21 software was used to construct a neighbor-joining tree based on 1,000 bootstrap replications<sup>[34]</sup>.

**Subcellular localization of *CsKTN1***

Full-length CDSs (coding sequences) of *CsKTN1* from CCMC and *mp* mutant alleles were fused with GFP (green fluorescent protein) in pGreen vector (the modified vector contains 35S and GFP fragments) to generate plant binary expression vector p35S::CsKTN1<sup>S</sup>(CCMC)-GFP and p35S::CsKTN1<sup>F</sup>(*mp*)-GFP. Restriction sites were included in primers to facilitate cloning and the corresponding fragments were cloned into SmaI-cut pGreen plasmid to produce p35S::Gene-GFP recombinant plasmids. Two recombinant plant expression plasmids and one free GFP plasmid p35S::GFP used as a positive control, were used for transient expression in tobacco leaf cells (4 weeks old) via agrobacterium (C58) infection. Agrobacterium was cultured overnight until OD<sub>600</sub> value = 1.0 and suspended with binding buffer (MgCl<sub>2</sub> 10 mmol·l<sup>-1</sup>, MES 10 mmol·l<sup>-1</sup>, Acetosyringone 200  $\mu\text{mol}\cdot\text{l}^{-1}$ , pH 5.6) after centrifugation. Agrobacterium was injected into tobacco leaves. Infected tobacco plants were kept in darkness at 27 °C for 2–3 d to allow transient expression of transgenes. Fluorescent signals were detected using a Zeiss LSM800 ultra high-resolution confocal microscope. The primer sequences are listed in Supplemental Table S1.

**Quantitative real-time PCR (qRT-PCR) analysis**

Quantitative real-time PCR (qRT-PCR) was performed on tissue samples from the first fully expanded true leaf, root, main stem of second internode, male and female flower at anthesis, tendril at 10-true-leaf stage from CCMC and *mp* plants. Roots were dug out of the soil and quickly frozen in liquid nitrogen. Total RNA was extracted with RNAPrep Plant Mini Kit (Tiangen) following the manufacturer's instructions. First strand cDNA was synthesized using Prime Script 1st Strand cDNA Synthesis Kit (TaKaRa). qRT-PCR was performed with a TB-GREEN Premix Ex Taq™ Kit (TaKaRa) in Bio-Rad CFX96 quantitative real-time PCR system, and the values of triplicate reactions were averaged. The threshold cycle (Ct) value of each gene was investigated and normalized to Ct value of *CsActin*. Relative mRNA expression data was analyzed using the 2<sup>- $\Delta\Delta\text{CT}$</sup>  method. The primer sequences are listed in Supplemental Table S1.

**Protein expression and purification**

Full length CDS of *CsKTN1<sup>C</sup>* (CCMC allele) and *CsKTN1<sup>T</sup>* (*mp* allele) were cloned into pCZN1 vector (His-tag) and expressed in Arctic Express™ bacteria (DE3). The IPTG (isopropyl  $\beta$ -D-1-thiogalactopyranoside) was used to induce protein expression. The expressed proteins were purified by Ni-IDA-Sefinose (TM) Resin (Novagen) following the manufacturer's instructions. Purified proteins were analyzed by 12% SDS-PAGE (sodium dodecyl sulfate polyacrylamide gel electrophoresis).

**Microtubule binding assay**

Microtubule coprecipitation test was performed to verify the binding relationship between target protein (*CsKTN1*) and microtubule *in vitro* as previously described<sup>[35]</sup>. Purified tubulin protein (Cytoskeleton, Porcine Brain, Cat. #T240) and target

proteins, CsKTN1<sup>S</sup> (CCMC allele)-His and CsKTN1<sup>F</sup> (*mp* allele)-His, were centrifuged at 200,000 *g* at 4 °C for 20 min before use. Two target proteins (PBS buffer dissolved) at a concentration of 2 μM were mixed with a 2 μM tubulin solution in binding buffer (100 mM PIPES, 1 mM MgCl<sub>2</sub>, 1 mM EGTA, 20 mM paclitaxel and 1 mM GTP, pH = 6.9), at room temperature for 30 min. After centrifugation at 100,000 *g* for 30 min, the pellets (resuspended by binding buffer) and supernatant were analyzed by SDS-PAGE.

### Microtubule shearing and observation

Rhodamine-labeled tubulin (Cytoskeleton, Porcine Brain, Cat. #TL590M) was polymerized in PEM binding buffer (100 mM PIPES, 1 mM MgCl<sub>2</sub>, 1 mM EGTA, pH = 6.9) containing 1 mM ATP and 20 mM taxol at 37 °C. Recombinant proteins CsKTN1<sup>S</sup>-His and CsKTN1<sup>F</sup>-His were diluted to the final concentration of 2 μM in PEM binding buffer and mixed with the polymerized tubulin (6 μM) at 37 °C for 30 min. The mixed proteins were fixed with 1% glutaraldehyde for observation by fluorescence microscopy.

## RESULTS

### Changes in cell morphology and size as determinants of the *micro-plant* mutant phenotype

From an EMS cucumber mutant library, a *micro-plant* (*mp*) mutant was identified showing miniaturized phenotypes in all organs (Fig. 1a–g). The plant height of *mp* mutant shrank significantly by ~80% of normal cucumber plant (CCMC) at the

expanded 10 true-leaf stage. Other organs such as hypocotyl, internode length, leaf size, ovary size and fruit length decreased by about 50% to 80% compared with that of CCMC (Supplemental Fig. S1). The *mp* mutant was female sterile hence unable to produce viable seeds. Specifically, there were fewer seeds in mature fruit of *mp* mutant, and all of them were empty, deflated and unable to germinate. The hybrid F<sub>1</sub> of CCMC and *mp* mutant displayed an intermediate phenotype, and its growth state was between CCMC and *mp* mutant (Fig. 1). In addition, the mutant also exhibited significant reduction of several key photosynthetic parameters (Pn, Gs, E and Fv/Fm) in *mp* mutant than CCMC (Supplemental Table S2).

Micro-structure of stem epidermal cells in *mp* mutant displayed irregular cell size and deformed cell shape compared with normal cucumber (Fig. 2). Triangle, trapezoid, or sub-circular cells were observed in *mp* mutant, while only long rhombus cells were observed in the normal plants (Fig. 2a, 2b). The length of epidermal cells in *mp* stem was significantly shorter than that of CCMC stem, while the width did not change significantly (Fig. 2c, 2d). In addition, the cell number of epidermal cells in *mp* stem was significantly increased (Fig. 2e). Paraffin sections of the ovary cells of *mp* mutant and CCMC were also examined, and the result showed that the ovary cells of mutant were smaller and irregularly arranged compared with CCMC (Supplemental Fig. S2). According to these findings, the emergence of *micro plant* phenotype was caused by changes in cell development and proliferation.

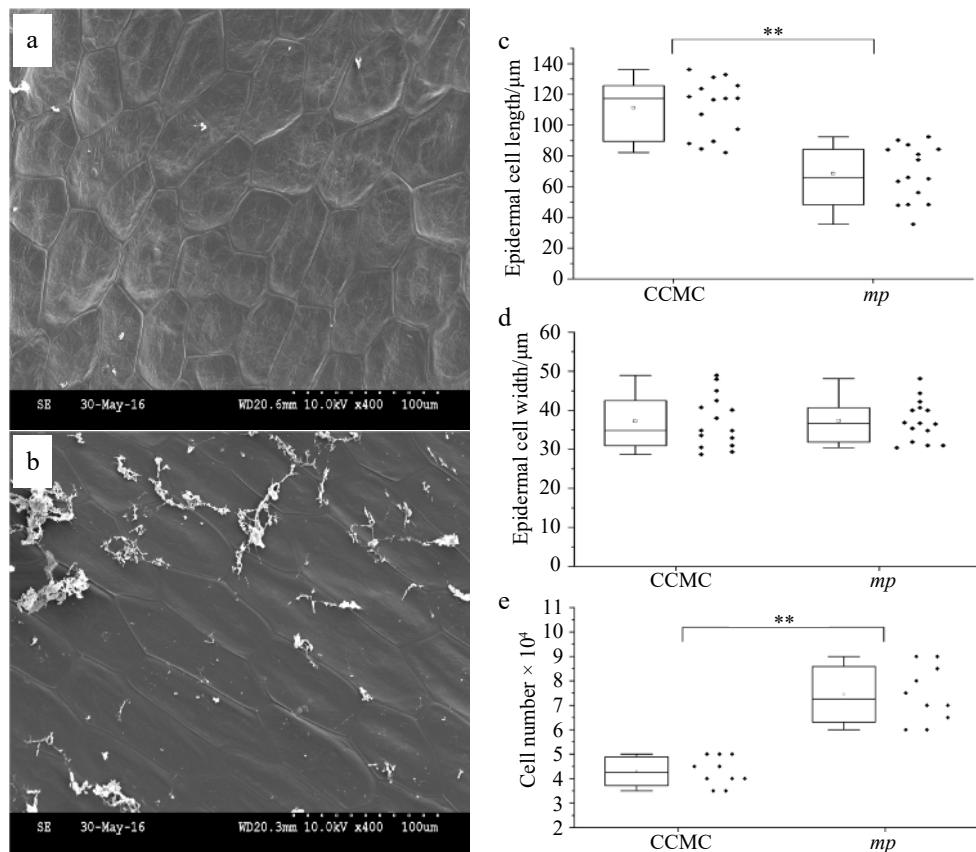


**Fig. 2** Scanning electron microscopy (SEM) observation of stem epidermal cells of CCMC and *mp* mutant. Micrographs of stem epidermal cells in (a) *mp* mutant and (b) CCMC. Scale bar = 100 μm. Boxplot indicating the (c) length, (d) width and (e) cell number of epidermal cells on stems of CCMC and *mp* mutant.

**Genetic mapping placed the *mp* locus to a 130.9 kb interval**

To explore the inheritance of *mp* phenotype, we developed F<sub>2</sub> population consisting of 485 plants derived from the cross between CCMC and *mp* mutant. 117, 255 and 113 plant individuals exhibited *micro-plant* type, intermediate type and normal plant phenotype in the F<sub>2</sub> population respectively, which fits the segregation ratio of 1:2:1 (*P* = 0.51). This suggested that the *micro-plant* mutant phenotype is controlled by a single gene with incomplete dominance.

From the F<sub>2</sub> plants, we bulked plants with extreme *micro-plant* and normal-plant phenotypes for re-sequencing. Each

pool has a sequencing depth of over 82.26 and coverage of over 93.43% (Supplemental Table S3). The potential polymorphisms were found by aligning the short reads of two bulks to CCMC consensus assembly. The calculated (SNP index) throughout the majority of the genome areas was 0.5, indicating that there was no substantial genetic variation between the two groups ( Fig. 3a ). A single genomic region harboring a cluster of SNPs with a high SNP index was identified in the 15.5–17.6 Mb interval of chromosome 7, suggesting that this candidate genomic region probably harbors the causative mutation ( Fig. 3a ).

For the low level of polymorphism between *mp* and CCMC at the candidate region, we developed another F<sub>2</sub> population

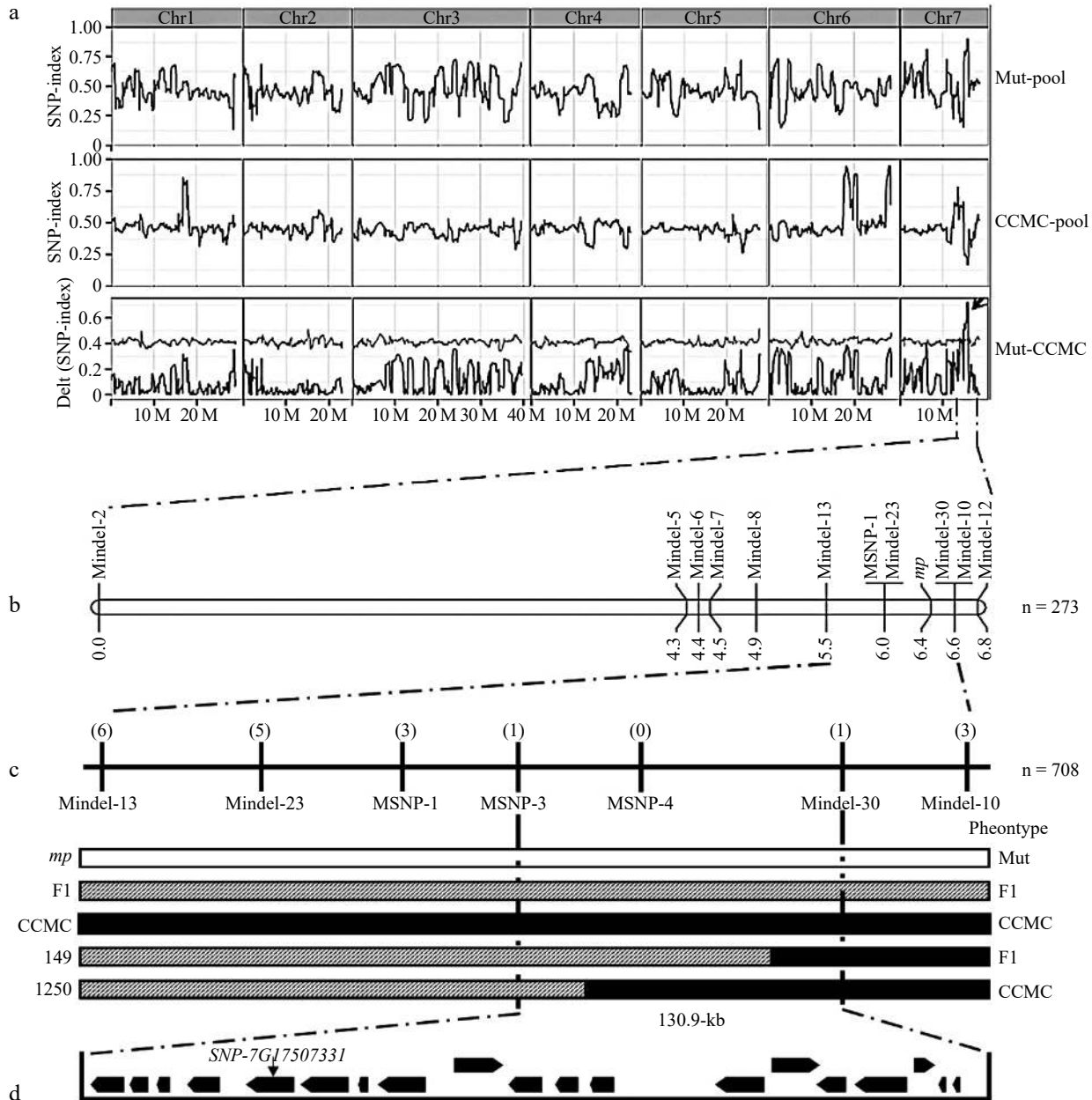


**Fig. 3** BSA-seq and linkage analysis of the *mp* locus. (a) BSA-seq analysis identified the candidate interval for *mp* locus to a 2.1 Mb genomic region harboring a high  $\Delta$ SNP index (subtracting the SNP-index value of the mutant-pool from the CCMC-pool) on chromosome 7 (15.5–17.6 Mb). (b) A genetic map based on a F<sub>2</sub> segregation population containing 273 individual plants delimited the *mp* locus to a 1.1 cM region. (c) Seven polymorphic markers and nine recombinants were applied to narrow down the *mp* locus to a 130.9 kb region. The numbers in parentheses indicate the number of recombinant plants of each marker. The white box indicates the mutant genotype, the black box for the CCMC genotype, and the striped box for the heterozygous genotype. (d) Genes (black boxes) and candidate mutation site in the mapping region.

(n = 273) from the cross between 'Hazerd' variety and *mp* mutant to narrow the potential region of *mp* locus. Ten polymorphic InDel markers and one SNP marker were developed between 'Hazerd' and *mp* mutant. After the marker genotypes of all 273 individuals were identified, an initial linkage map was constructed and *mp* locus was mapped to a 0.6 cM region flanking by two InDel markers (MIndel-23 and MIndel-10) (Fig. 3b). To identify more recombinants in this region, a larger F<sub>2</sub> population with 708 plants was examined, and two additional SNP markers were developed. Nine more recombinants were obtained, delimiting the *mp* locus into a 130.9 kb area flanked on Chr7 by markers MSNP-3 (17,480,086 bp) and MIndel-30 (17,611,033 bp) (Fig. 3c).

### A gene that encodes the Katanin p60 subunit protein was identified for *mp* locus

Nineteen genes were annotated in the 130.9 kb region (Fig. 3d, Supplemental Table S4). Based on the re-sequencing data of CCMC and two bulked pools, five SNPs were found in this region (Supplemental Table S5). Among these SNPs, SNP (*SNP-7G17507331*) causes a non-synonymous homozygous mutation (Supplemental Table S5). The other four SNPs were located in the intergenic region and had a low SNP index (below 0.6) in *mp* pool (Supplemental Table S5). There were no other base differences (like InDel or SV) in this region between two bulked pools. As a result, the *SNP-7G17507331* was considered as the causal SNP for the *mp* mutant.

According to the Cucumber Genome Database, *SNP-7G17507331* is located inside the gene *Csa7G435510* (Fig. 3d). We performed Sanger sequencing to clone the genomic and cDNA sequences of *Csa7G435510* from CCMC and *mp* mutant (Supplemental Fig. S3). The gene *Csa7G435510* consists of seven exons and encodes a Katanin p60 protein containing an AAA+-type ATPase domain of amino acid residues 225 to 514 (Fig. 4a, Supplemental Fig. S4). We named it as *CsKTN1*. The causal SNP at the exon 5 of *CsKTN1* resulted in an amino acid substitution from serine (S353) in CCMC to phenylalanine (F353) in *mp* mutant, which was located at the conserved AAA+-type ATPase domain, suggesting the potential modification in protein function (Fig. 4a, Supplemental Fig. S4).

To understand the structural and functional relationship among Katanin p60 homologs, we performed protein alignment and constructed a phylogenetic tree for *CsKTN1* with 9 Katanin p60 protein sequences from other crops (Supplemental Fig. S4). The alignment showed that AAA+-type ATPase domain is highly conserved across dicot and monocot plants. The similarity of *CsKTN1* to other Katanin p60 protein varied from 78% (*Arabidopsis* homolog) to 93.99% (*Melon* homolog). The phylogenetic tree showed that *CsKTN1* was clustered together with Katanin p60 protein from dicot species and far away from monocot crops (Fig. 4b).

Furthermore, we investigated the gene expression patterns of *CsKTN1* in various organs of *mp* and CCMC, including root, stem, leaf, male flower, ovary and tendril. The result showed that the expression level of *CsKTN1* was the highest in stem, followed by root, leaf, flower and tendril, and the lowest in ovary of CCMC. The expression level of *CsKTN1* gene was the highest in root, followed by tendril, leaf, stem and flower, and the lowest in ovary of *mp* mutant. Except for the tendril, the expression of *CsKTN1* was significantly lower in all organs of *mp* mutant compared to the CCMC (Fig. 4c). To characterize the gene function, we examined the subcellular localizations of the

protein encoded by two *CsKTN1* alleles (CCMC and *mp* mutant) in tobacco leaf epidermal cells. As a result, both *CsKTN1*-GFP fusion proteins (*CsKTN1*<sup>S</sup>(CCMC)-GFP and *CsKTN1*<sup>F</sup>(*mp*)-GFP) were localized in cell membrane, cytoplasm, and nucleus, similar to free GFP protein (Fig. 4d).

### The mutated *CsKTN1* protein lost part of its ability to bind and shear microtubule *in vitro*

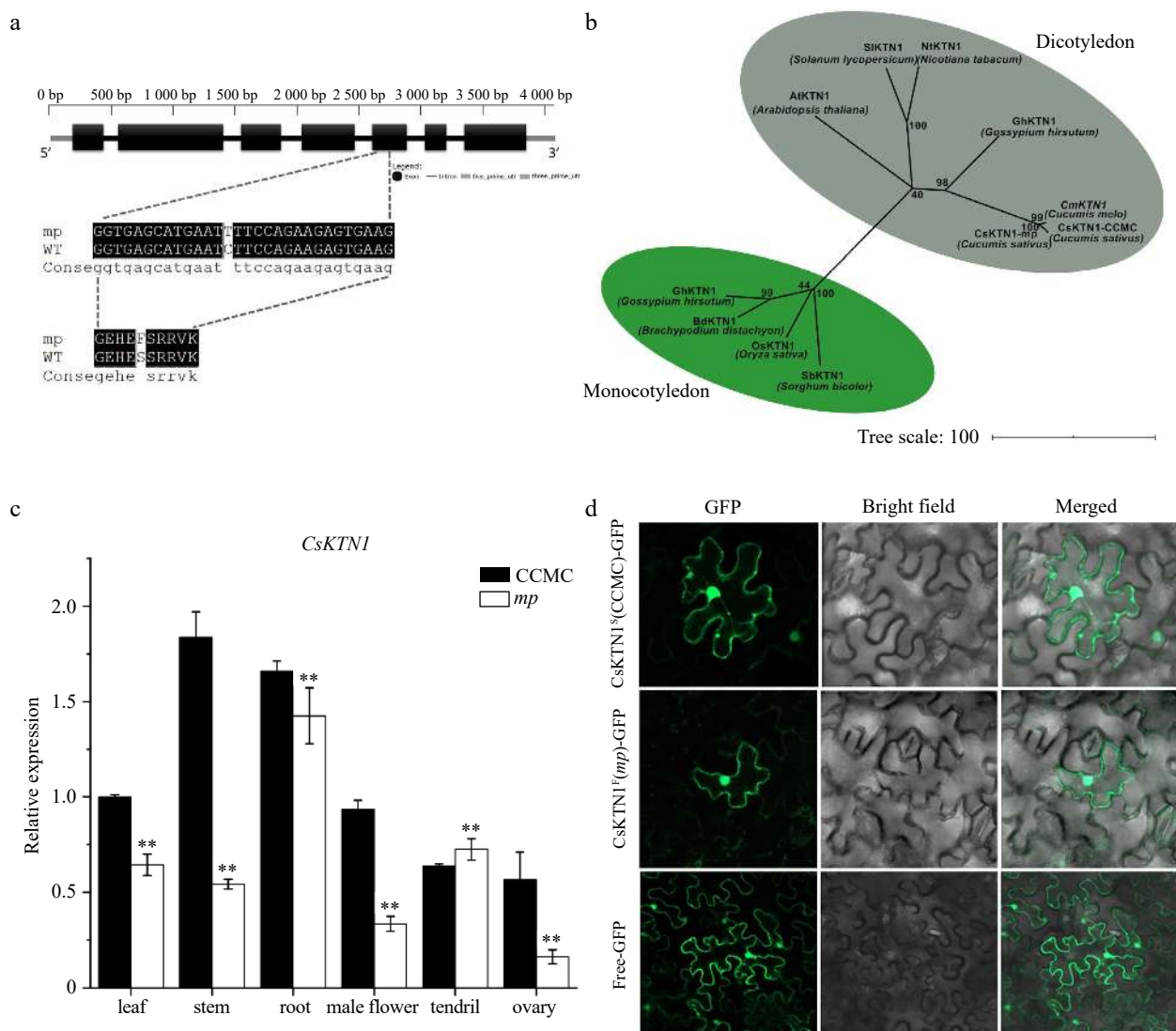
Given that Katanin p60 protein is required for microtubule-shearing in cell<sup>[17]</sup>, the molecular basis for *CsKTN1* in regulation of microtubule morphology was investigated *in vitro*. We applied the coprecipitation assay for two *CsKTN1*-His fusion proteins (CCMC and *mp*) to determine whether *CsKTN1* could bind to microtubule. As shown in Fig. 5a, in the absence of microtubules, none of the *CsKTN1*-His proteins was sedimented and retained in the supernatant. After incubation with microtubules, the amount of *CsKTN1*<sup>S</sup> (CCMC)-His in the pellets was found more than *CsKTN1*<sup>F</sup> (*mp* mutant)-His, indicating that *CsKTN1*<sup>S</sup> (CCMC)-His has a stronger ability to bind and coprecipitate with microtubules (Fig. 5a).

To investigate whether the microtubule-shearing function of *CsKTN1* was affected by amino substitution in *mp* mutant, we examined the shearing activity of *CsKTN1*<sup>S</sup>-His and *CsKTN1*<sup>F</sup>-His proteins. The taxol-stabilized and rhodamine-labeled microtubules were observed under fluorescence microscopy after perfusion with two recombinant proteins, *CsKTN1*<sup>S</sup>-His and *CsKTN1*<sup>F</sup>-His. As a result, *CsKTN1*<sup>S</sup>-His mediated complete microtubule shearing, while *CsKTN1*<sup>F</sup>-His mediated less rate of microtubule shearing *in vitro* (Fig. 5b). These results suggested that the amino acid substitution in the conserved domain of *CsKTN1* gene may affect the microtubules binding and shearing ability of target protein.

## DISCUSSION

Plant architecture is a key factor affecting photosynthetic efficiency and cultivation pattern of crops. Optimal plant architecture enables plant to have a superior form for light capture, which could boost planting density and increase the light energy utilization during the growth and development phase, hence improving the economic output<sup>[4,36]</sup>. Miniature or semi-dwarf wheat and rice varieties have been developed and cultivated worldwide, initiating a 'green revolution' in crop breeding and production<sup>[2,5]</sup>. In this study, a novel cucumber plant architecture mutant was identified from an EMS-induced mutagenesis population, which was regulated by Katanin p60 protein. The mutant with homologs *mp* locus exhibited extremely miniaturized phenotypes in various organs (Fig. 1). It also possesses both female sterile and male fertile characteristics, and the resultant offspring following the cross with normal cucumber plants in producing heterozygous *mp* locus showed potentially useful downsizing phenotypes (Fig. 1). Thus, it could be used not only as a good resource for cucumber hybrid production, but also as a good variety resource for vine length reduction, which might provide impetus for a new direction of breeding varieties with useful downsizing plant architecture to obtain better economic benefits.

Using BSA-seq and map-based cloning methods, we identified and cloned the causal gene (*Csa7G435510*) underlying cucumber *micro-plant* mutant (Fig. 3). *Csa7G435510* encodes a Katanin p60 protein that contains an AAA+-type ATPase domain which was highly conserved among homologous proteins from other species. Thus, it was designated as *CsKTN1*

The role of *CsKTN1* in cucumber

**Fig. 4** Identification of *CsKTN1* gene. (a) Diagram of the gene structure of *Csa7G435510*. A single-nucleotide mutation occurs in the fifth exon of *Csa7G435510* resulted in S (Serine) to F (Phenylalanine) substitution in *mp* mutant. (b) A neighbor-joining tree for cucumber Katanin p60 protein and its homologs with other selected plant species, constructed by MEGA 7. The numbers at the branch points represent bootstrap values (%) of 1000 replications. (c) Relative expression of *CsKTN1* in different tissues of *mp* and CCMC plants measured by qRT-PCR. Values are mean $\pm$ SD. \*\*  $P < 0.01$  (Student's *t*-test). (d) Subcellular localization of *CsKTN1* protein (CCMC and *mp* mutant) in tobacco epidermal cell. GFP signal was observed by confocal fluorescence microscopy. GFP, Bright field and Merged represent the images observed under different light fields. Free-GFP represents the free GFP plasmid p35S::GFP, while *CsKTN1*<sup>F</sup>(*mp*)-GFP and *CsKTN1*<sup>5</sup>(CCMC)-GFP represent two KTN1-GFP protein.

(Fig. 4a, 4b). A single nucleotide substitution (C1058T) in the coding region of *CsKTN1* leading to an amino acid substitution (S353F) was responsible for the plant miniatures (Fig. 4a, Supplemental Fig. S2). The mutation caused the down-regulation of *CsKTN1* in various tissues in the mutant except for the tendril (Fig. 4c). This may be due to the feedback effect of protein inactivation on gene transcription. This phenomenon of mutation in the coding sequence of gene rather than promoter region causing changes in gene expression has been reported in several mutants of cucumber<sup>[9–10,14]</sup>.

*CsKTN1* gene has been reported to control cucumber fruit length. A non-synonymous mutation of *CsKTN1* resulted in *short fruit3* (*sf3*) mutant<sup>[37]</sup>. The mutation sites of *CsKTN1* gene in *sf3* mutant and *mp* mutant are different, but the phenotypes of these two mutants are similar, such as shorter fruit, which confirmed the accuracy of *CsKTN1* as a candidate gene for *mp*

mutant. The ability of Katanin p60 protein to regulate plant morphology has great potential in the cultivation of diverse plant architecture varieties of cucumber.

Plant architectural modifications could be caused by the Katanin p60 mutation in other plants. In Arabidopsis, the Katanin p60 mutations, *fra2*, *Bot1* and *lue1*, showed the *micro-plant* phenotype<sup>[23,24,26]</sup>. In rice, the *dg1* mutant, a Katanin p60 mutation, exhibited dwarf, reduced organ size and short root phenotype<sup>[27]</sup>. In cotton, the Katanin-silenced plant showed dwarf phenotype with shorter internodes, and produced dark green and smaller leaf blades with shorter petioles<sup>[38]</sup>. Phylogenetic analysis showed that Katanin p60 proteins of cucumber had highly conserved domain and close evolutionary relationship with homologs proteins in other plants, implying that Katanin p60 homologs may share a regulatory function. However, phenotypic differences in *ktn1* mutations still exist in

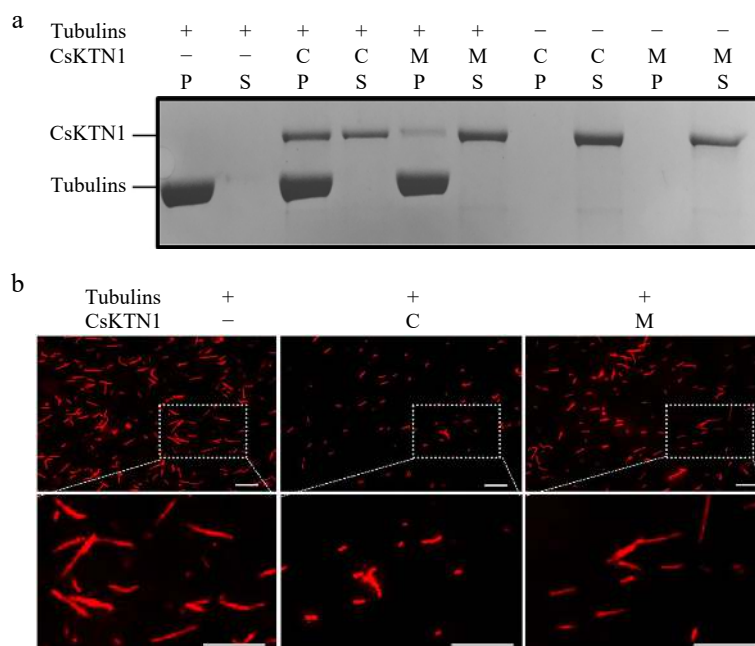


**Fig. 5** Microtubule binding and shearing capacity of CsKTN1. (a) Binding of CsKTN1 to microtubules *in vitro*. The proteins of supernatants (S) and the pellets (P) were analyzed on a coomassie-blue-stained polyacrylamide gel. C: CsKTN1<sup>S</sup> (CCMC)-His, M: CsKTN1<sup>F</sup> (*mp* mutant)-His, +: present, -: absent. (b) Microtubule-shearing activity of CsKTN1 *in vitro*. The shearing situation of microtubules was observed by fluorescence microscopy. Bar = 10  $\mu$ m.

different species. For example, in *Arabidopsis* and rice, *ktn1* decreased fertility and produced less fertile seeds compared to wild type<sup>[26,27]</sup>, while in cucumber, it resulted in female sterility with no active seeds. In addition, F<sub>1</sub> hybrids from the crosses of *ktn1* and wild type in cucumber and rice showed intermediate phenotypes (Fig. 1), indicating that mutant trait was regulated by an incomplete dominant gene<sup>[27]</sup>, while in *Arabidopsis*, the trait was regulated by a recessive gene<sup>[24]</sup>. These discrepancies could be caused by species differences or the different mutation sites in *KTN1* gene.

As the cytoskeleton, microtubules participate in a series of important life activities in cells, such as maintenance of cell structure, intracellular material transport, and mitosis<sup>[15]</sup>. The microtubules are in a state of controllable instability and dynamics, and are precisely regulated by the microtubule-associated protein (MAP) to maintain normal physiological functions of cells<sup>[39]</sup>. Several MAPs have been identified in plants and animals that are involved in promoting microtubule stabilization or destabilization<sup>[40]</sup>. The ability of Katanin p60 protein to bind and shear microtubules *in vitro* has also been found in *Arabidopsis*<sup>[16]</sup>. We confirmed that the CsKTN1 protein is a MAP by co-precipitation and microtubule shearing experiments (Fig. 5). In addition, the ability of CsKTN1 mutant protein to bind and shear microtubules decreased, indicating that the mutated amino acid has a negative impact on the function of CsKTN1 (Fig. 5). We speculate that the change of dynamic state of microtubules was the direct reason for the change of cell structure and eventually led to the change of plant architecture of the *mp* mutant.

In conclusion, we propose that a mutation in the *CsKTN1* gene encoding Katanin p60 protein caused the changes in cucumber plant architecture. The results obtained in this paper will be useful for elucidating the mechanisms of Katanin p60 protein regulating cucumber plant architecture.

## ACKNOWLEDGMENTS

This research was supported by the National Natural Science Foundation of China (31772318), the Fund for Independent Innovation of Agricultural Science and Technology of Jiangsu Province [CX(20)2019], the Key Research and Development Program (BE2021357 and 2021YFD1200201-04), Jiangsu Belt and Road innovation cooperation project (BZ2019012), and the Project Funded by the Priority Academic Program Development of Jiangsu Higher Education Institutions. And we thank Obel Hesbon and Marzieh Davoudi for polishing the language of the manuscript.

## Conflict of interest

The authors declare that they have no conflict of interest.

**Supplementary Information** accompanies this paper at (<http://www.maxapress.com/article/doi/10.48130/VR-2022-0003>)

## Dates

Received 22 October 2021; Accepted 11 February 2022; Published online 24 February 2022

## REFERENCES

- Zhao L, Tan L, Zhu Z, Xiao L, Xie D, et al. 2015. *PAY1* improves plant architecture and enhances grain yield in rice. *The Plant Journal* 83:528–36
- Chen S, Gao R, Wang H, Wen M, Xiao J, et al. 2015. Characterization of a novel reduced height gene (*Rht23*) regulating panicle morphology and plant architecture in bread wheat. *Euphytica* 203:583–94



The role of *CsKTN1* in cucumber

3. Pan Q, Xu Y, Li K, Peng Y, Zhan W, et al. 2017. The genetic basis of plant architecture in 10 maize recombinant inbred line populations. *Plant Physiology* 175:858–73
4. Wang Y, Li J. 2008. Molecular basis of plant architecture. *Annual Review of Plant Biology* 59:253–79
5. Monna L, Kitazawa N, Yoshino R, Suzuki J, Masuda H, et al. 2002. Positional cloning of rice semidwarfing gene, *sd-1*: rice "green revolution gene" encodes a mutant enzyme involved in gibberellin synthesis. *DNA Research* 9:11–17
6. Wang Y, Bo K, Gu X, Pan J, Li Y, et al. 2020. Molecularly tagged genes and quantitative trait loci in cucumber with recommendations for QTL nomenclature. *Horticulture Research* 7:3
7. Li Y, Yang L, Pathak M, Li D, He X, et al. 2011. Fine genetic mapping of *cp*: a recessive gene for compact (*dwarf*) plant architecture in cucumber, *Cucumis sativus* L. *Theoretical and Applied Genetics* 123:973–83
8. Lin T, Wang S, Zhong Y, Gao D, Cui Q, et al. 2016. A truncated f-box protein confers the dwarfism in cucumber. *Journal of Genetics and Genomics* 43:223–26
9. Hou S, Niu H, Tao Q, Wang S, Gong Z, et al. 2017. A mutant in the *CsDET2* gene leads to a systemic brassinosteroid deficiency and super compact phenotype in cucumber (*Cucumis sativus* L.). *Theoretical and Applied Genetics* 130:1693–703
10. Wang H, Li W, Qin Y, Pan Y, Wang X, et al. 2017. The cytochrome p450 gene *CsCYP85A1* is a putative candidate for *Super compact-1* (*Scp-1*) plant architecture mutation in cucumber (*Cucumis sativus* L.). *Frontiers in Plant Science* 8:266
11. Xu L, Wang C, Cao W, Zhou S, Wu T. 2018. CLAVATA1-type receptor-like kinase *CsCLAVATA1* is a putative candidate gene for *dwarf* mutation in cucumber. *Molecular Genetics and Genomics* 293:1393–405
12. Chen F, Fu B, Pan Y, Zhang C, Wen H, et al. 2017. Fine mapping identifies *CsGCN5* encoding a histone acetyltransferase as putative candidate gene for *tendrill-less1* mutation (*td-1*) in cucumber. *Theoretical and Applied Genetics* 130:1549–58
13. Gao D, Zhang C, Zhang S, Hu B, Wang S, et al. 2017. Mutation in a novel gene *SMALL AND CORDATE LEAF 1* affects leaf morphology in cucumber. *Journal of Integrative Plant Biology* 59:736–41
14. Yang L, Liu H, Zhao J, Pan Y, Cheng S, et al. 2018. *LITTLELEAF* (*LL*) encodes a WD40 repeat domain-containing protein associated with organ size variation in cucumber. *The Plant Journal* 95:834–47
15. Wasteneys GO. 2002. Microtubule organization in the green kingdom: chaos or self-order? *Journal of Cell Science* 115:1345–54
16. Stoppin-Mellet V, Gaillard J, Vantard M. 2003. Plant katanin, a microtubule severing protein. *Cell Biology International* 27:279
17. Hamada T. 2007. Microtubule-associated proteins in higher plants. *Journal of Plant Research* 120:79–98
18. Lin D, Cao L, Zhou Z, Zhu L, Ehrhardt D, et al. 2013. Rho GTPase signaling activates microtubule severing to promote microtubule ordering in Arabidopsis. *Current Biology* 23:290–97
19. Wan L, Wang X, Li S, Hu J, Huang W, et al. 2014. Overexpression of *OskTN80a*, a katanin P80 ortholog, caused the repressed cell elongation and stalled cell division mediated by microtubule apparatus defects in primary root in *Oryza sativa*. *Journal of Integrative Plant Biology* 56:622–34
20. Wang G, Wang C, Liu W, Ma Y, Dong L, et al. 2018. Augmin antagonizes katanin at microtubule crossovers to control the dynamic organization of plant cortical arrays. *Current Biology* 28:1311–1317.E3
21. Juranic M, Srilunchara KO, Krohn NG, Leljak-Levanic D, Sprunck S, et al. 2012. Germline-specific MATH-BTB substrate adaptor MAB1 regulates spindle length and nuclei identity in maize. *The Plant Cell* 24:4974–91
22. Luptovciak I, Samakovli D, Komis G, Samaj J. 2017. KATANIN 1 is essential for embryogenesis and seed formation in Arabidopsis. *Frontiers in Plant Science* 8:728
23. Bichet A, Desnos T, Turner S, Grandjean O, Höfte H. 2001. *BOTERO1* is required for normal orientation of cortical microtubules and anisotropic cell expansion in Arabidopsis. *The Plant Journal* 25:137–48
24. Burk DH, Liu B, Zhong R, Morrison WH, Ye Z. 2001. A katanin-like protein regulates normal cell wall Biosynthesis and cell elongation. *The Plant Cell* 13:807–27
25. Meier C, Bouquin T, Nielsen ME, Raventos D, Mattsson O, et al. 2001. Gibberellin response mutants identified by luciferase imaging. *The Plant Journal* 25:509–19
26. Bouquin T, Mattsson O, Naested H, Foster R, Mundy J. 2003. The Arabidopsis *lue1* mutant defines a katanin p60 ortholog involved in hormonal control of microtubule orientation during cell growth. *Journal of Cell Science* 116:791–801
27. Komorisono M, Ueguchi-Tanaka M, Aichi I, Hasegawa Y, Ashikari M, et al. 2005. Analysis of the rice mutant *dwarf and gladius leaf 1*. Aberrant katanin-mediated microtubule organization causes up-regulation of gibberellin biosynthetic genes independently of gibberellin signaling. *Plant Physiology* 138:1982–93
28. Nakamura M, Ehrhardt DW, Hashimoto T. 2010. Microtubule and katanin-dependent dynamics of microtubule nucleation complexes in the acentrosomal Arabidopsis cortical array. *Nature Cell Biology* 12:1064–70
29. Chen C, Liu M, Jiang L, Liu X, Zhao J, et al. 2014. Transcriptome profiling reveals roles of meristem regulators and polarity genes during fruit trichome development in cucumber (*Cucumis sativus* L.). *Journal of Experimental Botany* 65:4943–58
30. Liu X, Pan Y, Liu C, Ding Y, Wang X, et al. 2020. Cucumber fruit size and shape variations explored from the aspects of morphology, histology, and endogenous hormones. *Plants* 9:772
31. Abe A, Kosugi S, Yoshida K, Natsume S, Takagi H, et al. 2012. Genome sequencing reveals agronomically important loci in rice using MutMap. *Nature Biotechnology* 30:174–78
32. Song M, Cheng F, Wang J, Wei Q, Fu W, et al. 2019. A leaf shape mutant provides insight into PINOID Serine/Threonine Kinase function in cucumber (*Cucumis sativus* L.). *Journal of Integrative Plant Biology* 61:1000–14
33. Huang SW, Li RQ, Zhang ZH, Li L, Gu XF, et al. 2009. The genome of the cucumber, *Cucumis sativus* L. *Nature genetics* 41:1275–81
34. Saitou N, Nei M. 1987. The neighbor-joining method: a new method for reconstructing phylogenetic trees. *Molecular Biology and Evolution* 4:406–25
35. Zhang Q, Lin F, Mao T, Nie J, Yan M, et al. 2012. Phosphatidic acid regulates microtubule organization by interacting with MAP65-1 in response to salt stress in Arabidopsis. *The Plant Cell* 24:4555–76
36. Jiao Y, Wang Y, Xue D, Wang J, Yan M, et al. 2010. Regulation of *OsSPL14* by *OsmiR156* defines ideal plant architecture in rice. *Nature Genetic* 42:541–44
37. Wang H, Sun J, Yang F, Weng Y, Chen P, et al. 2021. *CsKTN1* for a katanin p60 subunit is associated with the regulation of fruit elongation in cucumber (*Cucumis sativus* L.). *Theoretical and Applied Genetics* 134:2429–2441
38. Qu J, Ye J, Geng Y, Sun Y, Gao S, et al. 2012. Dissecting functions of *KATANIN* and *WRINKLED1* in cotton fiber development by virus-induced gene silencing. *Plant Physiology* 160:738–48
39. Smertenko AP, Chang HY, Wagner V, Kaloriti D, Fenyk S, et al. 2004. The Arabidopsis microtubule-associated protein AtMAP65-1: molecular analysis of its microtubule bundling activity. *The Plant Cell* 16:2035–47
40. Krtkova J, Benakova M, Schwarzerova K. 2016. Multifunctional microtubule-associated proteins in plants. *Frontiers in Plant Science* 7:474



Copyright: © 2022 by the author(s). Published by Maximum Academic Press, Fayetteville, GA. This article is an open access article distributed under Creative Commons Attribution License (CC BY 4.0), visit <https://creativecommons.org/licenses/by/4.0/>.